Reduction in lipophilicity improved the solubility, plasma-protein binding, and permeability of tertiary sulfonamide RORc inverse agonists

17 AUTHORS, INCLUDING:

Yuzhong Deng
Genentech

36 PUBLICATIONS **740** CITATIONS

SEE PROFILE

Adam R Johnson
Genentech

42 PUBLICATIONS **919** CITATIONS

SEE PROFILE

Weiru Wang
Genentech

63 PUBLICATIONS **2,957** CITATIONS

SEE PROFILE

Reduction in lipophilicity improved the solubility, plasma–protein binding, and permeability of tertiary sulfonamide RORc inverse agonists

Benjamin P. Fauber [a,*], Olivier René [a], Gladys de Leon Boenig [a], Brenda Burton [b], Yuzhong Deng [a], Céline Eidenschenk [a], Christine Everett [a], Alberto Gobbi [a], Sarah G. Hymowitz [a], Adam R. Johnson [a], Hank La [a], Marya Liimatta [a], Peter Lockey [b], Maxine Norman [b], Wenjun Ouyang [a], Weiru Wang [a], Harvey Wong [a]

[a] Genentech, Inc., 1 DNA Way, South San Francisco, CA 94080, USA
[b] Argenta, Units 7-9 Spire Green Centre, Flex Meadow, Harlow, Essex CM19 5TR, UK

ABSTRACT

Using structure-based drug design principles, we identified opportunities to reduce the lipophilicity of our tertiary sulfonamide RORc inverse agonists. The new analogs possessed improved RORc cellular potencies with >77-fold selectivity for RORc over other nuclear receptors in our cell assay suite. The reduction in lipophilicity also led to an increased plasma–protein unbound fraction and improvements in cellular permeability and aqueous solubility.

© 2014 Elsevier Ltd. All rights reserved.

The cytokine interleukin (IL)-17 plays a central role in the pathogenesis of many inflammatory diseases including rheumatoid arthritis (RA),[1] multiple sclerosis (MS),[2] psoriasis,[3] and inflammatory bowel disease (IBD).[4] It has been demonstrated that the expression of IL-17 from T helper (T_H)-17 cells requires the expression of the nuclear receptor (NR) retinoic acid receptor-related orphan receptor gamma (RORγ or RORc, also known as NR1F3).[5] RORc is also indispensable for the production of IL-17 by innate lymphoid cells (ILCs)[6] and γδ T cells,[7] in addition to playing a role in the production of the proinflammatory cytokines IL-22[8] and granulocyte macrophage colony-stimulating factor (GM-CSF).[9] Based on RORc's influence over multiple inflammatory pathways, it has been suggested that small molecule regulators of this NR could potentially lead to anti-inflammatory therapeutics.[10,11] A recent series of publications illustrated that small molecule RORc inverse agonists were efficacious in a murine model of psoriasis,[12] a collagen-induced arthritis (CIA) mouse model for RA,[13,14] and the experimental autoimmune encephalomyelitis (EAE) mouse model

for MS.[14–17] This preclinical in vivo efficacy data has further validated RORc as a suitable target for the treatment of inflammatory disease.

A biochemical screening campaign at Genentech identified a series of tertiary sulfonamides as RORc inverse agonists (Fig. 1, Compounds **1** and **2**), which we disclosed in a previous publication.[18] In order to assist in the optimization of these tertiary sulfonamide lead molecules, we co-crystallized compound **1** with the human RORc ligand-binding domain (LBD) and obtained a 2.2 Å resolution X-ray structure.[19] The helices of the RORc-LBD co-structure adopted the canonical three-layered α-helical fold observed with previously reported RORc X-ray structures,[20] with **1** bound in the ligand binding pocket. The RORc-LBD crystallized with two protein molecules in the asymmetric unit, which were identical in conformation except for the relative order and placement of their *C*-termini (Supplementary data, Fig. S1a). In one monomer, only helix 12 was visualized at the interface of the asymmetric unit (Fig. S1b).[21] In the other monomer, the full *C*-terminus was packed against a neighboring protein molecule at the dimer interface (Fig. S1c). RORc inverse agonists can destabilize helices 11–12.[22,23] However, in the RORc-LBD co-structure with **1**,

* Corresponding author. Tel.: +1 650 467 5773.
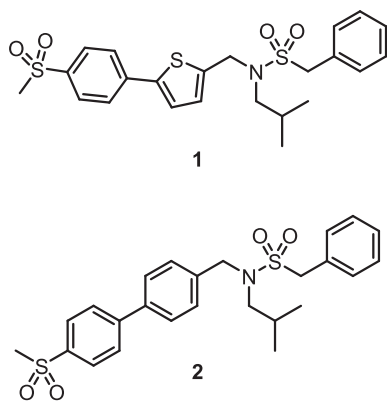 *E-mail address:* Fauber.Benjamin@gene.com (B.P. Fauber).

Figure 1. Tertiary sulfonamide RORc inverse agonist ligands reported by Genentech.

the C-terminal region was ordered and there were no direct interactions between **1** and the protein. Therefore, we assumed that crystal packing led to the ordering of the C-terminal residues.

The RORc-LDB environment and protein's interactions with **1** were identical in both monomers of the aforementioned asymmetric unit. The benzylic ring on the tertiary sulfonamide of **1** formed edge-to-face π–π interactions[24] with Trp317 (3.7 Å) and Phe486 (3.8 Å) (Fig. 2a). It was notable that His479 on helix 11 of the RORc-LBD did not adopt the same orientation that was observed in a previously reported RORc agonist ligand co-structure [PDB: 3L0L], in which His479 formed a hydrogen bond (3.0 Å) with Tyr502.[25] In the RORc-LBD co-structure with **1**, His479 engaged the benzylic ring of **1** in an edge-to-face π–π interaction (3.3 Å) (Fig. 2a), and prohibited it from forming the aforementioned hydrogen bond with Tyr502 on helix 12. The ligand-induced movement of His479 may account for the RORc inverse agonist profile of **1** and the disorder and/or loss of secondary structure for helices 11′–12 in the RORc-LBD co-structure. The orientation and interactions of His479 have been previously postulated by our group[23] and others[22] as an important regulator of RORc function. The N-isobutyl group of **1** resided in a shallow lipophilic pocket lined with Val376, Phe388, Ile400, and Phe401. The central thiophene ring of **1** hovered over Met365 and participated in a sulfur–arene interaction[26] (4.6 Å). The thiophene ring of **1** also participated in an edge-to-face π–π interaction with Phe378 (4.2 Å). The interactions of the thiophene ring on **1** with the RORc ligand binding pocket account for the tight SAR observed with the thiophene ring replacements we described in a previous publication.[18] The para-methanesulfonyl group of **1** resided in the hydrophilic region of the RORc ligand binding pocket and **1** formed a weak hydrogen bond[26] with Arg367 (3.5 Å) and a water-mediated hydrogen bond (3.1 Å) to Tyr281 (2.7 Å) and the backbone carbonyl of Cys285 (2.8 Å) (Fig. 2b). It was also noted that **1** resided in the RORc ligand binding pocket in a very different orientation than the previously described co-structure of T0901713 (N-(4-(1,1,1,3,3,3-hexafluoro-2-hydroxypropan-2-yl)phenyl)-N-(2,2,2-trifluoroethyl)benzenesulfonamide) with the RORc-LBD [PDB: 4NB6],[23] and there were limited opportunities to bridge the SAR between these two distinct classes of RORc inverse agonist ligands.

An evaluation of **1** in a panel of in vitro assays revealed that it had low aqueous solubility (≤1 μM at pH 7.4), high plasma–protein binding (PPB) (99% bound in both human and rodent serum), and low apparent permeability (P_{app}) as assessed by the Madin-Darby canine kidney (MDCK)[27] cell assay ($P_{app(A \rightarrow B)} = 2 \times 10^{-6}$ cm/s).[28] In our evaluation of the X-ray co-structure of **1** with the RORc-LBD, it was evident that several features on **1** were interacting with the RORc ligand binding pocket. Yet the terminal arene ring in the biaryl motif of **1** only served as a spacer to orient the para-methanesulfonyl moiety toward the aforementioned
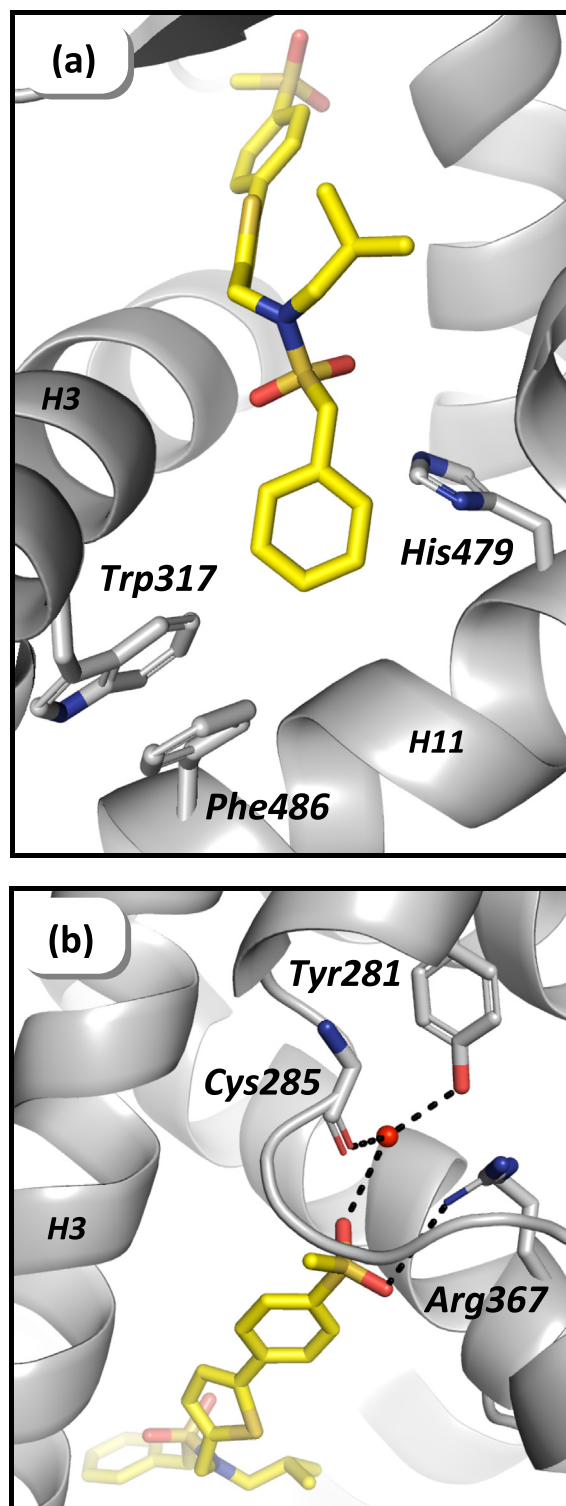

Figure 2. A 2.2 Å resolution co-crystal structure of compound **1** (yellow) in complex with the RORc-LDB (grey) [PDB: 4QM0]. Water molecules are spheres (red) and hydrogen bonds are dashed lines (black). Side chain residues have been omitted for clarity. (a) The benzylic ring of the tertiary sulfonamide formed edge-to-face π–π interactions with His479 (grey, 3.3 Å), Phe486 (grey, 3.8 Å), and Trp317 (grey, 3.7 Å). (b) The para-methanesulfonyl moiety of **1** made a direct hydrogen bond (3.5 Å) with Arg367 (grey) and a water-mediated hydrogen bond (3.1 Å) to Tyr281 (grey, 2.7 Å) and the backbone carbonyl of Cys285 (grey, 2.8 Å).

hydrogen bonding interaction partners in the protein. Therefore, we sought to replace the terminal arene in the biaryl motif of **2** with a suitable non-aromatic heterocycle.[29] Such a change would

decrease the aromatic ring count (#Ar) and could increase the solubility while lowering the PPB.[30] It would also lower the lipophilicity[31] of our chemical series and increase the fraction of sp[3]-hybridized carbons (Fsp^3), which could potentially improve the solubility.[32] A reduction in lipophilicity, as assessed by the measured $\log P$ or calculated $\log P$ ($c \log P$) values, can lead to improvements in cellular permeability and aqueous solubility[33,34] while also decreasing PPB[35] and minimizing any potential secondary pharmacology associated with our molecules.[36,37]

Aryl-piperazines and aryl-piperidines are proven biaryl isosteres.[38] With this consideration in mind, we initiated a campaign to replace the terminal arene of **2** with a range of substituted piperazines and piperidines. The analogs were synthesized via the Buchwald–Hartwig amination reaction[39] and an aryl-bromide tertiary sulfonamide advanced intermediate.[40] The analogs were tested in a time-resolved fluorescence biochemical assay that monitored the ability of the human RORc-LBD to bind to a co-activator peptide derived from steroid receptor co-activator-1 (SRC1).[41] Compounds that disrupted the recruitment of the SRC1 co-activator peptide were RORc inverse agonists.[20]

Replacement of the terminal arene on **2** with an *N*-methanesulfonyl-piperazine (**3**) demonstrated that the change was tolerated, with only a 10-fold loss in RORc inverse agonist potency while also reducing the $c \log P$[42] value by 1.6 log units (Table 1). Homologation of the sulfonamide functional group one atom outside of the ring (**4**) provided a molecule that was equipotent (RORc SRC1 EC_{50} = 20 nM) to **2** and less lipophilic. Removal of the sulfonamide nitrogen in **4** provided sulfone analog **5** which was of similar potency (RORc SRC1 EC_{50} = 42 nM). The collective results of analogs **3**–**5** demonstrated that the orientation and distance of the sulfone moiety in relation to Arg367 could be important for potency, but the sulfonamide N–H was not making any essential hydrogen bonding interactions with the hydrophilic region of the ligand binding pocket. To further explore the position of the sulfone moiety, a 1,1-dioxothiomorpholine analog (**6**) was synthesized because it had an improved $c \log P$ value versus the exocyclic sulfone analog (**5**) ($c \log P$ = 2.3 and 3.7, respectively). Compound **6** was approximately 20-fold less potent than **5**, further illustrating the importance of the appropriately positioned sulfonyl group to interact with the RORc ligand binding pocket. It was also noted that compounds **2**–**6** all contained multiple sulfonamide/sulfone functional groups, and all of the compounds had low aqueous solubility values (⩽1 μM at pH 7.4).[43] To explore the relationship of sulfones/sulfonamides and solubility, we focused on other functional groups in an effort to maintain the potency of **2** while improving the aqueous solubility of subsequent analogs. The morpholine analog (**7**) was modestly potent in the RORc SRC1 co-activator peptide recruitment assay (EC_{50} = 0.21 μM), and it was also more potent than the corresponding 1,1-dioxothiomorpholine analog (**6**). This result indicated that the sulfone or sulfonamide group might not be the optimal functional group on the aliphatic heterocyclic ring in the hydrophilic region of the RORc ligand binding pocket. Consequently, we also explored a variety of functional groups. Compound **8** was less potent in the SRC1 co-activator assay, relative to **7**, whereas **9** demonstrated improvements in potency (EC_{50} = 0.10 μM) and aqueous solubility. Methylation of the hydroxyl group on **9** resulted in the retention of RORc inverse agonist potency and a reduction in aqueous solubility (Compound **10**, EC_{50} = 0.16 μM). Introduction of a nitrile moiety at the 4-position of the piperidine (**11**) provided a further improvement in RORc inverse agonist potency, as did the introduction of a primary amide (**12**). Compound **12** was quite promising since it was less lipophilic than **2**, yet it had similar activity in the RORc SRC1 co-activator peptide recruitment assay (EC_{50} = 70 nM). We explored other variants of this functional group such as the tertiary amide analog (**13**), which was approximately 10-fold less active than **12**. The *N*-acyl

piperazine group (**14**) led to a molecule with additional RORc potency (EC_{50} = 57 nM) and an equivalent $c \log P$ value to **12**. The methyl carbamate analog (**15**) was a less potent RORc inverse agonist than **14**, and homologation of the amide functional group outside of the ring (**16**) also resulted in a loss of potency. In summary, the exploration of the heterocyclic aliphatic *N*-linked rings identified the amide functionality in **14** as an optimal combination of RORc inverse agonist potency and decreased lipophilicity relative to the starting molecule (**2**). The notable drawback in this endeavor was the lack of improvement in aqueous solubility values for most analogs. Thus, we turned our attention to the *N*-alkyl substituent in an effort to make further reductions in lipophilicity and potential improvements in aqueous solubility.

As discussed earlier in the analysis of the X-ray co-structure of **1** with the RORc-LBD, the *N*-isobutyl group of the ligand resided in a shallow lipophilic pocket but did not appear to make any specific interactions with the protein. With this consideration in mind, we sought to explore a variety of *N*-alkyl groups that could maintain or increase the potency of analogs, relative to **14**, while also lowering the lipophilicity. The *N*-alkyl analogs were synthesized by either (1) alkylation of a secondary sulfonamide advanced intermediate or (2) introduction of the bulkier *N*-alkyl groups early in the synthesis then carrying the molecules through several standard transformations to reveal the final compounds.[40] Introduction of the *N*-cyclobutyl group (Table 2, Compound **17**) led to an approximate two-fold improvement in the RORc inverse agonist potency (EC_{50} = 30 nM) while also decreasing the $c \log P$ value 0.2 log units and increasing the aqueous solubility (37 μM). Synthesis of the *tert*-butyl isomer (**18**) resulted in a compound that was equipotent to **17**, yet less soluble (⩽1 μM) and more lipophilic. Replacement of the *iso*-butyl group with a 3-oxetane ring (**19**) led to a substantial loss of RORc potency (EC_{50} = 4.9 μM) with improvements in solubility (189 μM) and lipophilicity. Introduction of the *n*-propyl, *i*-propyl, and *c*-propyl *N*-alkyl groups (compounds **20**–**22**) were all well tolerated (EC_{50} = 70, 37, 100 nM, respectively), and most also provided notable improvements in lipophilicity and aqueous solubility. The ethyl (**23**) and 2,2,2-trifluoroethyl (**24**) analogs also possessed favorable RORc inverse agonist potencies (EC_{50} = 94 and 13 nM, respectively) while also displaying improved solubility and lipophilicity profiles over **14**. Polar functional groups such as methoxyethyl (**25**) and *N,N*-dimethylaminoethyl (**26**) were poorly tolerated in the lipophilic pocket of the RORc protein as were the methyl (**27**) and methylenecyano (**28**) moieties. The results of compounds **19** and **25**–**28** illustrated the tight SAR in the shallow lipophilic pocket of the protein occupied by the isobutyl group on **1** (ergo **14**), as aliphatic or halogenated aliphatic moieties of a certain size were the only tolerated *N*-alkyl substituents. The SAR of the benzylic sulfonamide group on the right-hand side of the molecule was also explored with a variety of aliphatic and heteroaromatic sulfonamide replacements. Ultimately, there were no notable improvements over the parent benzylic sulfonamide group (data not shown).

We analyzed the potent RORc inverse agonist compounds identified with the SRC1 co-activator recruitment assay in a panel of HEK293 cell Gal4-ROR construct reporter assays. We profiled three known isoforms of human ROR (RORc, RORb, and RORa) by monitoring the suppression of their basal transcriptional activity in the absence of any exogenous agonist.[41] In order to assess the NR cellular selectivity of the potent RORc inverse agonists, we also tested these compounds in cellular reporter assays of human farnesoid X receptor (FXR), liver X receptor (LXR)-α, LXRβ, and pregnane X receptor (PXR) in both agonist mode (no agonist ligand added) and antagonist mode (using T0901317 as an exogenous ligand).[41]
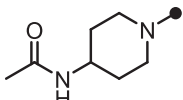
In our NR cellular assays, we found **2** was a modestly potent RORc inverse agonist (RORc cell EC_{50} = 0.45 μM) with only four-fold selectivity over the other NRs in our assay panel (Table 3,

Table 1
Structure–activity relationships of the 4-benzylic substituents
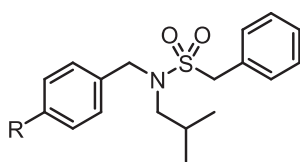
Compd	R-group	RORc SRC1 EC$_{50}$[a] (µM) [%eff.]	$c\log P$[b]	RORc LLE[c]	Solubility[d] (µM)
2		0.025 [−94%]	4.5	3.0	⩽1
3		0.21 [−92%]	2.9	4.0	⩽1
4		0.020 [−96%]	4.1	3.2	⩽1
5		0.042 [−93%]	3.7	3.3	⩽1
6		0.70 [−89%]	2.3	4.2	⩽1
7		0.21 [−90%]	3.8	2.6	⩽1
8		2.3 [−75%]	4.0	2.3	60
9		0.10 [−97%]	4.2	2.4	7
10		0.16 [−92%]	4.7	2.1	⩽1
11		0.074 [−96%]	4.2	2.8	⩽1
12		0.070 [−95%]	3.5	3.4	⩽1
13		0.86 [−90%]	4.2	1.7	⩽1
14		0.057 [−96%]	3.5	3.8	⩽1
15		0.31 [−92%]	4.2	2.3	⩽1

Table 1 (*continued*)

Compd	R-group	RORc SRC1 EC$_{50}$[a] (µM) [%eff.]	$c\log P$[b]	RORc LLE[c]	Solubility[d] (µM)
16		0.92 [−84%]	3.9	2.3	⩽1

All assay results are reported as the geometric mean of at least two separate runs.[41]

[a] Inhibition of RORc LBD recruitment of a peptide derived from the SRC1 co-activator protein; negative percent efficacy '%eff.' denotes inverse agonism relative to the basal activity of apo-RORc LBD in this assay format.
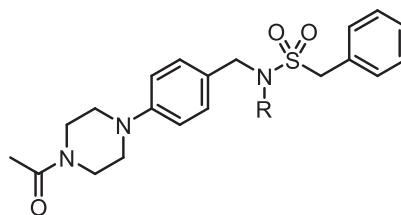
[b] Calculated log P ($c\log P$) value.[42]

[c] Ligand-Lipophilicity Efficiency (LLE)[46] was calculated using the RORc SRC1 EC$_{50}$ and the $c\log P$.

[d] Aqueous kinetic solubility at pH 7.4.

Table 2
Structure–activity relationships of the *N*-alkyl R-groups

Compd	R-group	RORc SRC1 EC$_{50}$[a] (µM) [%eff.]	$c\log P$[b]	RORc LLE[c]	Solubility[d] (µM)
17	*c*-Bu	0.030 [−97%]	3.2	4.3	37
18	*t*-Bu	0.029 [−97%]	3.4	3.8	⩽1
19	3-Oxetane	4.9 [−73%]	1.8	3.4	189
20	*n*-Pr	0.070 [−95%]	3.2	3.6	40
21	*i*-Pr	0.037 [−98%]	3.0	4.0	⩽1
22	*c*-Pr	0.10 [−97%]	2.8	4.1	71
23	Et	0.094 [−98%]	2.7	4.2	31
24	CH$_2$CF$_3$	0.013 [−98%]	3.0	4.5	5
25	(CH$_2$)$_2$OMe	0.68 [−87%]	2.1	4.1	87
26	(CH$_2$)$_2$NMe$_2$	>10	2.2	—	221
27	Me	5.1	2.2	3.2	7
28	CH$_2$CN	6.5	1.8	3.5	125

All assay results are reported as the geometric mean of at least two separate runs.[41]

[a] Inhibition of RORc LBD recruitment of a peptide derived from the SRC1 co-activator protein; negative percent efficacy '%eff.' denotes inverse agonism relative to the basal activity of apo-RORc LBD in this assay format.

[b] Calculated log P ($c\log P$) value.[42]

[c] Ligand-Lipophilicity Efficiency (LLE)[46] was calculated using the RORc SRC1 EC$_{50}$ and the $c\log P$.

[d] Aqueous kinetic solubility at pH 7.4.

Table 3
RORc potency and selectivity profiles in Gal4 human transcription assays[a]

Compd	RORc Cell EC$_{50}$ (µM)	RORb Cell EC$_{50}$ (µM)	RORa Cell EC$_{50}$ (µM)	FXR Cell EC$_{50}$ (µM)	LXRα Cell EC$_{50}$ (µM)	LXRβ Cell EC$_{50}$ (µM)	PXR Cell EC$_{50}$ (µM)
2	0.45	2.5	2.4	2.4	2.3	2.5	3.0
14	0.12	>10	>10	>10	>10	>10	>10
17	0.13	>10	>10	>10	>10	>10	>10
21	0.41	1.2	>10	>10	>10	>10	>10
24	0.27	>10	>10	>10	>10	>10	>10

All assay results are reported as the geometric mean of at least two separate runs.

[a] All assays were conducted in HEK293-Gal4 cellular constructs. All NR assays monitored the suppression of their respective basal transcriptional activities, an outcome consistent with inverse agonist activity of ligands with these receptors.[41]

EC$_{50}$ values = 2.4–3.0 µM). We were pleased to see that the RORc biochemical potency observed with compounds **14** and **17** translated to favorable RORc cellular potencies (EC$_{50}$ values = 0.12 and 0.13 µM, respectively). Additionally, these compounds were more selective for RORc versus the other NRs in our selectivity panel, exhibiting a >77-fold selectivity for RORc. Compound **21** was less potent and selective for RORc than **17** in the ROR cellular assays, and it harbored some affinity for RORb (RORc cell EC$_{50}$ = 0.41 µM, RORb cell EC$_{50}$ = 1.2 µM). Compound **24** also exhibited a favorable RORc potency (RORc cell EC$_{50}$ = 0.27 µM) and selectivity profile, with >37-fold selectivity for RORc over the other NRs in our assay

panel. None of the compounds exhibited agonist activity in the FXR, LXR, and PXR activation cell assays (data not shown). Only compound **14** exhibited PXR agonist activity (EC$_{50}$ = 0.50 µM, 25-fold activation versus the T0901317 control).

Additionally, we progressed compounds **14**, **17**, and **24** into human peripheral blood mononuclear cell (PBMC) cytokine production assays to assess their abilities to inhibit the production of IL-17 (Table 4).[41] Compounds **14** and **17** displayed modest inhibition of IL-17 production in the human PBMC assay (EC$_{50}$ = 0.77 and 0.80 µM, respectively), while compound **24** was slightly less potent (EC$_{50}$ = 0.97 µM). The differences in IL-17 inhibition values

Table 4
Potency in human IL-17 and INFγ production assays[a]

Compd	IL-17 PBMC EC$_{50}$ (μM)	IL-17 PBMC%max. inhibition (%)	IFNγ EC$_{50}$ (μM)	CTG EC$_{50}$ (μM)
14	0.77	80	>10	>10
17	0.80	95	>10	>10
24	0.97	81	>10	>10

All assay results are reported as the geometric mean of at least two separate runs.
[a] All assays were conducted using peripheral blood mononuclear cells (PBMCs) isolated from human whole blood.[41] Interferon gamma (INFγ) and CellTiter-Glo® (CTG) cell culture assays were used as positive controls to monitor for non-T$_H$17 cell cytokine activity and adverse off-target effects on cell physiology, respectively.[41]

Table 5
In vitro ADME properties of compounds **2** and **17**

Compd	Human PPB[a] (%unbound)	Rat PPB[a] (%unbound)	MDCK[b] P_{app} A → B (10^{-6} cm/s)	MDCK[b] P_{app} B → A (10^{-6} cm/s)
2	1	1	3	2
17	6	6	24	24

See the Supplementary data for experimental details associated with each assessment.
[a] Plasma–protein binding (PPB).
[b] Apparent membrane permeability (P_{app}) in a Madin-Darby canine kidney (MDCK) cell permeability assay.

between the three compounds exhibited roughly the same trend in potency observed in the RORc Gal4 cellular assay. It was also noteworthy that none of the compounds showed any activity in the interferon (INF)-γ or CellTitler-Glo® (CTG) assays,[41] demonstrating that the compounds were not indiscriminately suppressing cytokine production, nor were they grossly cytotoxic.

We also profiled compound **17** against a panel of in vitro assays to determine if the reduction in lipophilicity versus **2** translated to improvements in the in vitro ADME properties.[44] Compound **17** displayed a six-fold increase in the PPB unbound fraction in human and rodent serum when compared to **2** (Table 5).[28] Additionally, **17** demonstrated an eight-fold improvement in cellular permeability over **2**, as assessed by the MDCK cell assay ($P_{app(A→B)}$ = 24 x 10^{-6} cm/s).[28] We also found that **17** did not inhibit the major cytochrome P450 (CYP) isoforms up to compound concentrations of 10 μM.[45] When **17** was incubated with human and rat liver microsomes, it displayed high hepatic clearance (Cl$_{hep}$) values (>70% of liver blood flow for both species), thus the utility of **17** may be limited to in vitro studies.

In conclusion, we employed structure-based drug design principles to optimize the biaryl region of our tertiary sulfonamide series into an aryl-piperazine motif. Optimized analog **17** possessed improved RORc inverse agonist cell potencies versus the starting point, and >77-fold selectivity for RORc over other NRs as assessed by cellular assays. The improvements in RORc cellular potency translated into inhibition of IL-17 production in a human PBMC assay. A concomitant reduction in lipophilicity (as assessed by $c\log P$ values) translated into improved solubility, plasma-protein unbound fraction, and cellular permeability for the tertiary sulfonamide series.

Acknowledgments

Supplementary data

Supplementary data associated with this article can be found, in the online version, at http://dx.doi.org/10.1016/j.bmcl.2014.06.048.

References and notes

1. Chabaud, M.; Durand, J. M.; Buchs, N.; Fossiez, F.; Page, G.; Frappart, L.; Miossec, P. *Arthritis Rheum.* **1999**, *42*, 963.
2. Lock, C.; Hermans, G.; Pedotti, R.; Brendolan, A.; Schadt, E.; Garren, H.; Langer-Gould, A.; Strober, S.; Cannella, B.; Allard, J.; Klonowski, P.; Austin, A.; Lad, N.; Kaminski, N.; Galli, S. J.; Oksenberg, J. R.; Raine, C. S.; Heller, R.; Steinman, L. *Nat. Med.* **2002**, *8*, 500.
3. Rich, P.; Sigurgeirsson, B.; Thaci, D.; Ortonne, J.-P.; Paul, C.; Schopf, R. E.; Morita, A.; Roseau, K.; Harfst, E.; Guettner, A.; Machacek, M.; Papavassilis, C. *Br. J. Dermatol.* **2013**, *168*, 402.
4. Fujino, S.; Andoh, A.; Bamba, S.; Ogawa, A.; Hata, K.; Araki, Y.; Bamba, T.; Fujiyama, Y. *Gut* **2003**, *52*, 65.
5. Ivanov, I. I.; McKenzie, B. S.; Zhou, L.; Tadokoro, C. E.; Lepelley, A.; Lafaille, J. J.; Cua, D. J.; Littman, D. R. *Cell* **2006**, *126*, 1121.
6. Eberl, G.; Marmon, S.; Sunshine, M.-J.; Rennert, P. D.; Choi, Y.; Littman, D. R. *Nat. Immunol.* **2004**, *5*, 64.
7. Pantelyushin, S.; Haak, S.; Ingold, B.; Kulig, P.; Heppner, F. L.; Navarini, A. A.; Becher, B. *J. Clin. Invest.* **2012**, *122*, 2252.
8. Sabat, R.; Ouyang, W.; Wolk, K. *Nat. Rev. Drug Disc.* **2014**, *13*, 21.
9. Codarri, L.; Gyülvészi, G.; Tosevski, V.; Hesske, L.; Fontana, A.; Magnenat, L.; Suter, T.; Becher, B. *Nat. Immunol.* **2011**, *12*, 560.
10. Huang, Z.; Xie, H.; Wang, R.; Sun, Z. *Expert Opin. Ther. Targets* **2007**, *11*, 737.
11. Huh, J. R.; Littman, D. R. *Eur. J. Immunol.* **2012**, *42*, 2232.
12. Skepner, J.; Ramesh, R.; Trocha, M.; Schmidt, D.; Baloglu, E.; Lobera, M.; Carlson, T.; Hill, J.; Orband-Miller, L. A.; Barnes, A.; Boudjelal, M.; Sundrud, M.; Ghosh, S.; Yang, J. *J. Immunol.* **2014**, *192*, 2564.
13. Chang, M. R.; Lyda, B.; Kamenecka, T. M.; Griffin, P. R. *Arthritis Rheum.* **2014**, *66*, 579.
14. Wang, Y.; Cai, W.; Zhang, G.; Yang, T.; Liu, Q.; Cheng, Y.; Zhou, L.; Ma, Y.; Cheng, Z.; Lu, S.; Zhao, Y.-G.; Zhang, W.; Xiang, Z.; Wang, S.; Yang, L.; Wu, Q.; Orband-Miller, L. A.; Xu, Y.; Zhang, J.; Gao, R.; Huxdorf, M.; Xiang, J.-N.; Zhong, Z.; Elliott, J. D.; Leung, S.; Lin, X. *Bioorg. Med. Chem.* **2014**, *22*, 692.
15. Huh, J. R.; Leung, M. W. L.; Huang, P.; Ryan, D. A.; Krout, M. R.; Malapaka, R. R. V.; Chow, J.; Manel, N.; Ciofani, M.; Kim, S. V.; Cuesta, A.; Santori, F. R.; Lafaille, J. J.; Xu, H. E.; Gin, D. Y.; Rastinejad, F.; Littman, D. R. *Nature* **2011**, *472*, 486.
16. Solt, L. A.; Kumar, N.; Nuhant, P.; Wang, Y.; Lauer, J. L.; Liu, J.; Istrate, M. A.; Kamenecka, T. M.; Roush, W. R.; Vidović, D.; Schürer, S. C.; Xu, J.; Wagoner, G.; Drew, P. D.; Griffin, P. R.; Burris, T. P. *Nature* **2011**, *472*, 491.
17. Xu, T.; Wang, X.; Zhong, B.; Nurieva, R. I.; Ding, S.; Dong, C. *J. Biol. Chem.* **2011**, *286*, 22707.
18. Fauber, B. P.; René, O.; Burton, B.; Everett, C.; Gobbi, A.; Hawkins, J.; Johnson, A. R.; Liimatta, M.; Lockey, P.; Norman, M.; Wong, H. *Bioorg. Med. Chem. Lett.* **2014**, *24*, 2182.
19. See the Supplementary data for the experimental details associated with the co-crystal structure of the RORc-LBD with compound **1**. The coordinates and structure factors for the complex between RORc and compound **1** have been deposited with the protein data bank and assigned the accession code 4QM0.
20. Fauber, B. P.; Magnuson, S. *J. Med. Chem.* **2014**, 57. http://dx.doi.org/10.1021/jm401901d.
21. A similar observation was made in the co-structure of the RORc-LBD with digoxin [PDB: 3B0W] in which there was partial electron density in the region near helices 3–4 that suggested a small α-helix, composed of helix 12 residues, resided at the crystal packing interface. See Ref. 22 for additional details.
22. Fujita-Sato, S.; Ito, S.; Isobe, T.; Ohyama, T.; Wakabayashi, K.; Morishita, K.; Ando, O.; Isono, F. *J. Biol. Chem.* **2011**, *286*, 31409.
23. Fauber, B. P.; Boenig, G.; Burton, B.; Eidenschenk, C.; Everett, C.; Gobbi, A.; Hymowitz, S. G.; Johnson, A. R.; Liimatta, M.; Lockey, P.; Norman, M.; Ouyang, W.; René, O.; Wong, H. *Bioorg. Med. Chem. Lett.* **2013**, *23*, 6604.

24. Salonen, L. M.; Ellermann, M.; Diederich, F. *Angew. Chem., Int. Ed.* **2011**, *50*, 4808.
25. Jin, L.; Martynowski, D.; Zheng, S.; Wada, T.; Xie, W.; Li, Y. *Mol. Endocrinol.* **2010**, *24*, 923.
26. Bissantz, C.; Kuhn, B.; Stahl, M. *J. Med. Chem.* **2010**, *53*, 5061.
27. Irvine, J. D.; Takahashi, L.; Lockhart, K.; Cheong, J.; Tolan, J. W.; Selick, H. E.; Grove, J. R. *J. Pharm. Sci.* **1999**, *88*, 28.
28. See the Supplementary Data for the aqueous solubility, plasma protein binding, MDCK cellular permeability, and liver microsome stability assay protocols.
29. Our optimization campaign originated from compound **2** since our prior publication (see Ref. 18) demonstrated that **2** was superior to **1**.
30. Ritchie, T. J.; Macdonald, S. J. F. *Drug Discovery Today* **2009**, *14*, 1011.
31. Ritchie, T. J.; Macdonald, S. J. F.; Young, R. J.; Pickett, S. D. *Drug Discovery Today* **2011**, *16*, 164.
32. Ishikawa, M.; Hashimoto, Y. *J. Med. Chem.* **2011**, *54*, 1539.
33. Hill, A. P.; Young, R. J. *Drug Discovery Today* **2010**, *15*, 648.
34. Waring, M. J. *Expert Opin. Drug Discov.* **2010**, *5*, 235.
35. Trainor, G. L. *Expert Opin. Drug Discov.* **2007**, *2*, 51.
36. Leeson, P. D.; Springthorpe, B. *Nat. Rev. Drug Disc.* **2007**, *6*, 881.
37. Hughes, J. D.; Blagg, J.; Price, D. A.; Bailey, S.; DeCrescenzo, G. A.; Devraj, R. V.; Ellsworth, E.; Fobian, Y. M.; Gibbs, M. E.; Gilles, R. W.; Greene, N.; Huang, E.; Krieger-Burke, T.; Loesel, J.; Wager, T.; Whiteley, L.; Zhang, Y. *Bioorg. Med. Chem. Lett.* **2008**, *18*, 4872.
38. Wendt, M. D.; Shen, W.; Kunzer, A.; McClellan, W. J.; Bruncko, M.; Oost, T. K.; Ding, H.; Joseph, M. K.; Zhang, H.; Nimmer, P. M.; Ng, S.-C.; Shoemaker, A. R.; Petros, A. M.; Oleksijew, A.; Marsh, K.; Bauch, J.; Oltersdorf, T.; Belli, B. A.; Martineau, D.; Fesik, S. W.; Rosenberg, S. H.; Elmore, S. W. *J. Med. Chem.* **2006**, *49*, 1165.
39. Jiang, L.; Buchwald, S. Palladium-Catalyzed Aromatic Carbon-Nitrogen Bond Formation. In *Metal-Catalyzed Cross-Coupling Reactions*, 2nd ed.; de Meijere, A., Diederich, F., Eds.; Wiley-VCH GmbH & Co. KGaA: Weinheim, 2004; Vol. 2, pp 699–760.
40. For representative synthetic protocols and characterization of the analogs, see Fauber, B. P.; René, O. WO 2013/092941.
41. See the Supplementary Data section of Ref. 23 for the biochemical and cellular assay protocols.
42. The partition coefficient (log *P*) was calculated with internal software using the VolSurf approach. For additional details, see Cruciani, G.; Crivori, P.; Carrupt, P.-A.; Testa, B. J. *Mol. Struct. -Theochem.* **2000**, *503*, 17.
43. Total polar surface area (TPSA) has been shown to correlate with aqueous solubility, as described in (a) Faller, B.; Ertl, P. *Adv. Drug Delivery Rev.* **2009**, *59*, 533; The rationale behind this correlation was discussed further in (b) Ali, J.; Camilleri, P.; Brown, M. B.; Hutt, A. J.; Kirton, S. B. *J. Chem. Inf. Model.* **2012**, *52*, 420; Compounds **2–6** in Table 1 had higher TPSA values (91–116), calculated using the method described in (c) Ertl, P.; Rohde, B.; Selzer, P. *J. Med. Chem.* **2000**, *43*, 3714. as compared to compounds 17–27 in Table 2 (TPSA = 69–78).
44. In vitro assays to explore the themes of cellular permeability and predicted metabolic clearance have been referred to as in vitro ADME assays. For additional discussion, see Tarbit, M. H.; Berman, J. *Curr. Opin. Chem. Biol.* **1998**, *2*, 411.
45. CYP in vitro assay panel included the following isoforms: CYP3A4, CPY2C9, CYP2D6, CPY2C19, and CYP1A2.
46. See Ref. 36 and Leach, A. R.; Hann, M. M.; Burrows, J. N.; Griffen, E. J. *Mol. BioSyst.* **2006**, *2*, 429.